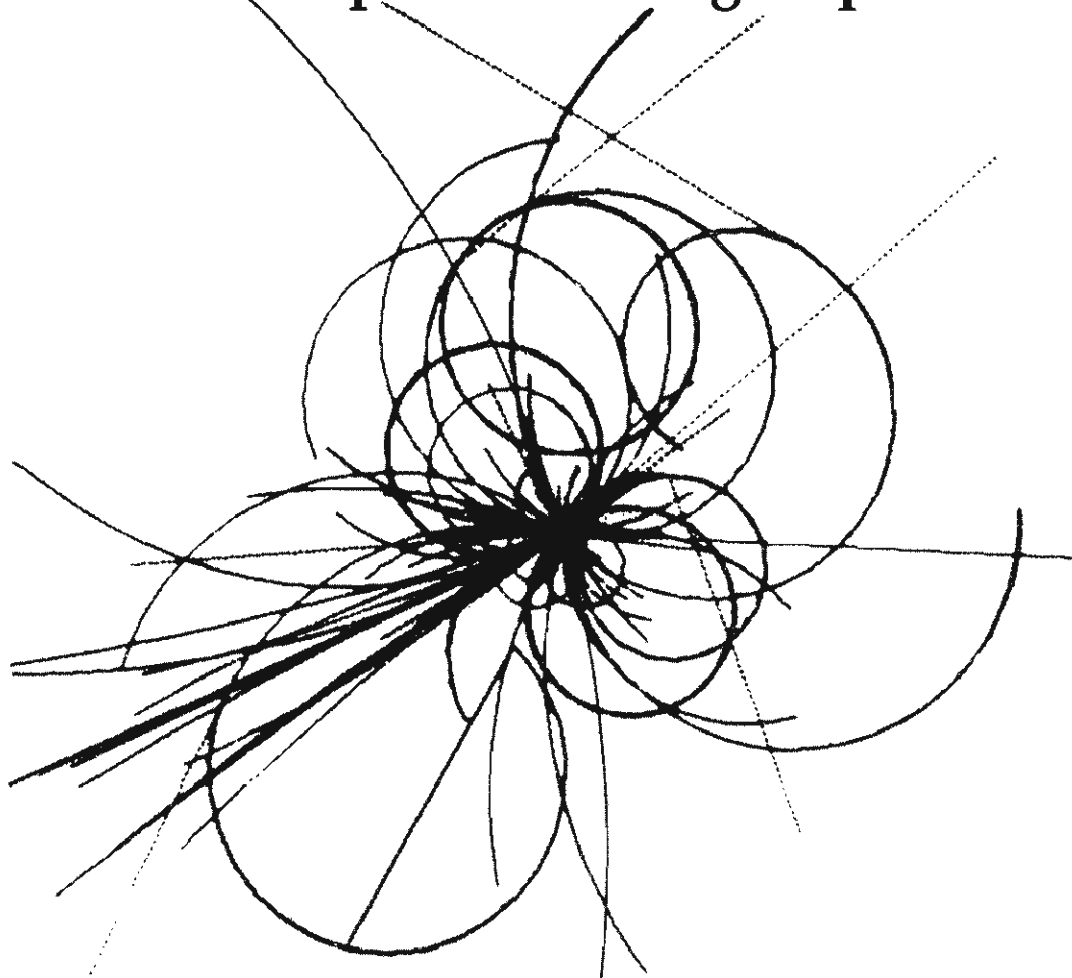


The Superconducting Super Collider



Opening the High-Energy Frontier

**Chris Quigg
SSC Central Design Group**

December 1988

OPENING THE HIGH-ENERGY FRONTIER*

Chris Quigg
SSC Central Design Group[†]
c/o Lawrence Berkeley Laboratory, Berkeley, California 94720

December 1988

*Talk given at the Symposium on Hadronic Matter in Collision, Tucson, Arizona, October 6-12, 1988, to appear in the Proceedings.

[†]Operated by the Universities Research Association, Inc., for the Department of Energy.

OPENING THE HIGH-ENERGY FRONTIER

CHRIS QUIGG

SSC CENTRAL DESIGN GROUP
LAWRENCE BERKELEY LABORATORY
BERKELEY, CA 94720 USA

1. ABSTRACT

I review the scientific motivation for an experimental assault on the 1-TeV scale, elaborating the idea of technicolor as one interesting possibility for what may be found there. I then summarize some of the discovery possibilities opened by a high-luminosity, multi-TeV proton-proton collider. After a brief résumé of the experimental environment anticipated at the SSC, I report on the status of the SSC R&D effort and discuss the work to be carried out over the course of the next year.

2. WHY THE SSC?

For more than a decade we have understood the importance of exploring interactions among the fundamental constituents at energies of about 1 TeV. Our expectations for what might be found there have been modulated by scientific fashions and informed by the progress of experimental technique, but the 1-TeV scale has remained an ever-fixed mark. If the scientific need for a step to much higher energies was already apparent, in broad terms, in the late 1970s, it has required sustained effort to develop the technical means to take that step. Formal studies of the feasibility of a multi-TeV accelerator began with workshops sponsored by ICFA at Fermilab in 1978 and at CERN in 1979. The idea of the SSC began to take shape during the Summer Study on Elementary Particle Physics and Future Facilities organized by the Division of Particles and Fields of the American

Physical Society at Snowmass in 1982 and was elaborated in workshops on accelerator and detector issues held during 1983 at Cornell and LBL. Encouraged by the successful operation of the Fermilab Tevatron, the 1983 HEPAP Subpanel on Future Facilities recommended "the immediate initiation of a multi-TeV, high-luminosity proton-proton collider project with the goal of physics at the earliest possible date." That recommendation may be taken as the beginning of the SSC project.

2.1 Why There Must Be New Physics on the 1-TeV Scale

Let us review the essential elements of the Weinberg-Salam $SU(2)_L \otimes U(1)_Y$ model of the weak and electromagnetic interactions. For brevity, I shall speak of the model as it applies to leptons. In this form, the model is neither complete nor consistent: anomaly cancellation requires that a doublet of color-triplet quarks must accompany each doublet of color-singlet leptons. However, the needed generalizations are simple enough that they need not be written out.

We begin by specifying the fermions: a left-handed weak-isospin doublet

$$L = \begin{pmatrix} \nu_e \\ e \end{pmatrix}_L \quad (2.1)$$

with weak hypercharge $Y_L = -1$, and a right-handed weak-isospin singlet

$$R = e_R \quad (2.2)$$

with weak hypercharge $Y_R = -2$.

The electroweak gauge group, $SU(2)_L \otimes U(1)_Y$, implies two sets of gauge fields: a weak isovector \vec{b}_μ , with coupling constant g , and a weak isoscalar \mathcal{A}_μ , with coupling constant $g'/2$. Corresponding to these gauge fields are the field-strength tensors $\vec{F}_{\mu\nu}$ for the weak-isospin symmetry and $f_{\mu\nu}$ for the weak-hypercharge symmetry.

We may summarize the interactions by the Lagrangian

$$\mathcal{L} = \mathcal{L}_{gauge} + \mathcal{L}_{leptons} \quad (2.3)$$

with

$$\mathcal{L}_{gauge} = -\frac{1}{4}F_{\mu\nu}^I F_I^{\mu\nu} - \frac{1}{4}f_{\mu\nu}f^{\mu\nu} , \quad (2.4)$$

and

$$\begin{aligned} \mathcal{L}_{leptons} = & \bar{R}i\gamma^\mu \left(\partial_\mu + i\frac{g'}{2}\mathcal{A}_\mu Y \right) R \\ & + \bar{L}i\gamma^\mu \left(\partial_\mu + i\frac{g'}{2}\mathcal{A}_\mu Y + i\frac{g}{2}\vec{\tau} \cdot \vec{b}_\mu \right) L . \end{aligned} \quad (2.5)$$

To hide the electroweak symmetry, we introduce a complex doublet of scalar fields

$$\phi = \begin{pmatrix} \phi^+ \\ \phi^0 \end{pmatrix} \quad (2.6)$$

with weak hypercharge $Y_\phi = +1$. Add to the Lagrangian new terms for the interaction and propagation of the scalars,

$$\mathcal{L}_{scalar} = (\mathcal{D}_\mu \phi)^\dagger (\mathcal{D}^\mu \phi) , \quad (2.7)$$

where the gauge-covariant derivative is

$$\mathcal{D}_\mu = \partial_\mu + i\frac{g'}{2}\mathcal{A}_\mu Y + i\frac{g}{2}\vec{\tau} \cdot \vec{b}_\mu , \quad (2.8)$$

and the potential interaction has the form

$$V(\phi^\dagger \phi) = \mu^2(\phi^\dagger \phi) + |\lambda|(\phi^\dagger \phi)^2 . \quad (2.9)$$

We are also free to add a Yukawa interaction between the scalar fields and the leptons:

$$\mathcal{L}_{Yukawa} = -G_e \left[\bar{R}(\phi^\dagger L) + (\bar{L}\phi)R \right] . \quad (2.10)$$

The electroweak symmetry is spontaneously broken if the parameter $\mu^2 < 0$. The minimum energy, or vacuum state, may be chosen to correspond to the vacuum expectation value

$$\langle \phi \rangle_0 = \begin{pmatrix} 0 \\ v/\sqrt{2} \end{pmatrix}, \quad (2.11)$$

where

$$v = \sqrt{-\mu^2/|\lambda|} \approx (G_F\sqrt{2})^{-1/2} \approx 246 \text{ GeV} \quad (2.12)$$

is fixed by the low-energy phenomenology of charged-current interactions.

The spontaneous symmetry breaking has several important consequences:

- Electromagnetism is mediated by a massless photon, coupled to the electric charge.
- The mediator of the charged-current weak interaction acquires a mass characterized by $M_W^2 = \pi\alpha/G_F\sqrt{2} \sin^2\theta_W$, where θ_W is the weak mixing angle.
- The mediator of the neutral-current weak interaction acquires a mass characterized by $M_Z^2 = M_W^2 / \cos^2\theta_W$.
- A massive neutral scalar particle, the Higgs boson, appears, but its mass is not predicted.
- Fermions (the electron in this abbreviated treatment) can acquire mass.

The standard model just outlined is incomplete;¹⁾ it does not explain how the scale of electroweak symmetry breaking is maintained in the presence of quantum corrections. The problem of the scalar sector can be summarized economically as follows.²⁾

Beyond the classical approximation, scalar mass parameters receive quantum corrections involving loops of particles of spins $J = 1, 1/2$, and 0 :

$$m^2(p^2) = m_0^2 + \underbrace{\text{---} \text{wavy} \text{---}}_{J=1} + \underbrace{\text{---} \text{loop} \text{---}}_{J=1/2} + \underbrace{\text{---} \text{circle} \text{---}}_{J=0} \quad (2.13)$$

The loop integrals are potentially divergent. Symbolically, we may summarize the content of (2.13) as

$$m^2(p^2) = m^2(\Lambda^2) + Cg^2 \int_{p^2}^{\Lambda^2} dk^2 + \dots , \quad (2.14)$$

where Λ defines a reference scale at which the value of m^2 is known, g is the coupling constant of the theory, and C is a constant of proportionality, calculable in any particular theory. Instead of dealing with the relationship between observables and parameters of the Lagrangian, we choose to describe the variation of an observable with the momentum scale. For the mass shifts induced by radiative corrections to remain under control (i.e., not to greatly exceed the value measured on the laboratory scale), either (i) Λ must be small, so the range of integration is not enormous, or (ii) new physics must intervene to cut off the integral.

In the standard $SU(3)_c \otimes SU(2)_L \otimes U(1)_Y$ model, the natural reference scale is the Planck mass,

$$\Lambda \sim M_{Planck} \approx 10^{19} \text{ GeV} . \quad (2.15)$$

In a unified theory of the strong, weak, and electromagnetic interactions, the natural scale is the unification scale,

$$\Lambda \sim M_U \approx 10^{15} \text{ GeV} . \quad (2.16)$$

Both estimates are very large compared with the scale of electroweak symmetry breaking (2.12). We are therefore assured that new physics must intervene at an energy of approximately 1 TeV, in order that mass shifts not be much larger than (2.12).

Only a few distinct classes of scenarios for controlling the contribution of the integral in (2.14) can be envisaged. The supersymmetric solution^{3]} is especially elegant. Exploiting the fact that fermion loops contribute with an overall minus sign (because of Fermi statistics), supersymmetry balances the contributions of fermion and boson loops. In the limit of unbroken supersymmetry, in which the masses of bosons are degenerate with those of their fermion counterparts, the cancellation is exact:

$$\sum_{\substack{i = \\ \text{fermions} \\ + \text{bosons}}} C_i \int dk^2 = 0 . \quad (2.17)$$

If the supersymmetry is broken (as it must be in our world), the contribution of the integrals may still be acceptably small if the fermion-boson mass splittings ΔM are not too large. The condition that $g^2\Delta M^2$ be “small enough” leads to the requirement that mass splittings, and hence superpartner masses, be less than about $1 \text{ TeV}/c^2$.

A second solution to the problem of the broad range of integration in (2.14) is offered by theories of dynamical symmetry breaking, such as technicolor.^{4]} In the technicolor scenario, the Higgs boson is composite, and new physics arises on the scale of its binding, $\Lambda_{TC} \approx 1 \text{ TeV}$. Thus the effective range of integration is cut off, and mass shifts are under control.

A third (and minimalist) possibility, which entails the sacrifice of perturbation theory for the electroweak interactions, is that of a strongly interacting gauge sector.^{5]} This would give rise to WW resonances, multiple production of Higgs bosons, and other new phenomena.

Nature may choose any (or none) of these human inventions, but we are driven unavoidably to the conclusion that some new physics must be found on the 1-TeV scale.

2.2 The Technicolor Alternative

Having reviewed some of the arguments for elaborating upon the standard model, I now consider one example of several possible extensions: the technicolor scheme of dynamical symmetry breaking. I select this in part because the other leading candidate, supersymmetry, is so well known, and in part because I find its claim on our attention very powerful.

We are not looking for a replacement of the standard model; we expect that the standard model will remain as the low-energy limit of a more complete theory, much as the four-fermion description of the charged-current weak interaction emerges as the low-energy limit of the Weinberg-Salam model.

2.2.1 The idea of technicolor. The dynamical symmetry-breaking approach, of which technicolor theories are exemplars, is modeled upon our understanding of another manifestation of spontaneous symmetry breaking in nature, the superconducting phase transition. The macroscopic order parameter of the Ginzburg-Landau phenomenology^{6]} corresponds to the wave

function of superconducting charge carriers. It acquires a nonzero vacuum expectation value in the superconducting state. The microscopic Bardeen-Cooper-Schrieffer theory^{7]} identifies the dynamical origin of the order parameter with the formation of collective states of elementary fermions, the Cooper pairs of electrons. The basic idea of the technicolor mechanism is to replace the elementary Higgs boson of the standard model by a fermion-antifermion bound state. By analogy with the superconducting phase transition, the dynamics of the fundamental technicolor gauge interactions among technifermions generate scalar bound states, and these play the role of the Higgs fields.

In the case of superconductivity, the elementary fermions (electrons) and the gauge interactions (QED) needed to generate the scalar bound states are already present in the theory. Could we achieve a scheme of similar economy for the electroweak symmetry-breaking transition?

Consider an $SU(3)_c \otimes SU(2)_L \otimes U(1)_Y$ theory of massless up and down quarks. Because the strong interaction is strong, and the electroweak interaction is feeble, we may consider the $SU(2)_L \otimes U(1)_Y$ interaction as a perturbation. For vanishing quark masses, QCD has an exact $SU(2)_L \otimes SU(2)_R$ chiral symmetry. At an energy scale $\sim \Lambda_{QCD}$, the strong interactions become strong, fermion condensates appear, and the chiral symmetry is spontaneously broken

$$SU(2)_L \otimes SU(2)_R \rightarrow SU(2)_V \tag{2.18}$$

to the familiar strong-interaction flavor (isospin) symmetry. Three Goldstone bosons appear, one for each broken generator of the original chiral invariance. These were identified by Nambu^{8]} as three massless pions.

The broken generators are three axial currents whose couplings to pions are measured by the pion decay constant f_π . When we turn on the $SU(2)_L \otimes U(1)_Y$ electroweak interaction, the electroweak gauge bosons couple to the axial currents and acquire masses of order $\sim gf_\pi$. The massless pions thus disappear from the physical spectrum, having become the longitudinal components of the weak gauge bosons. This achieves much of what we desire. Unfortunately, the mass acquired by the intermediate bosons is far smaller than required for a successful low-energy phenomenology; it is only^{9]}

$$M_W \approx 30 \text{ MeV}/c^2 . \quad (2.19)$$

2.2.2 A minimal model. The simplest transcription of these ideas to the electroweak sector is the minimal technicolor model of Weinberg^{10]} and Susskind.^{11]} The technicolor gauge group is taken to be $SU(N)_{TC}$ (usually $SU(4)_{TC}$), so the gauge interactions of the theory are generated by

$$SU(4)_{TC} \otimes SU(3)_c \otimes SU(2)_L \otimes U(1)_Y . \quad (2.20)$$

The technifermions are a chiral doublet of massless color singlets

$$\begin{pmatrix} U \\ D \end{pmatrix}_L \quad U_R \quad D_R . \quad (2.21)$$

With the electric charge assignments $Q(U) = \frac{1}{2}$ and $Q(D) = -\frac{1}{2}$, the theory is free of electroweak anomalies. The ordinary fermions are all technicolor singlets.

In analogy with our discussion of chiral symmetry breaking in QCD, we assume that the chiral TC symmetry is broken,

$$SU(2)_L \otimes SU(2)_R \otimes U(1)_V \rightarrow SU(2)_V \otimes U(1)_V . \quad (2.22)$$

Three would-be Goldstone bosons emerge. These are the technipions

$$\pi_T^+ \quad \pi_T^0 \quad \pi_T^- , \quad (2.23)$$

for which we are free to *choose* the technipion decay constant as

$$F_\pi = (G_F \sqrt{2})^{-1/2} = 247 \text{ GeV} . \quad (2.24)$$

When the electroweak interactions are turned on, the technipions become the longitudinal components of the intermediate bosons, which acquire masses

$$\begin{aligned} M_W^2 &= g^2 F_\pi^2 = \pi \alpha / G_F \sqrt{2} \sin^2 \theta_W \\ M_Z^2 &= (g^2 + g'^2) F_\pi^2 = M_W^2 / \cos^2 \theta_W \end{aligned} \quad (2.25)$$

that have the canonical standard model values, thanks to our choice (2.24) of the technipion decay constant.

Working by analogy with QCD, we may guess the spectrum of other $F\bar{F}$ bound states as follows:

$$\left. \begin{array}{l}
 1^{--} \text{ technirhos} \quad \rho_T^+ \quad \rho_T^0 \quad \rho_T^- \\
 1^{--} \text{ techniomega} \quad \omega_T \\
 0^{-+} \text{ technieta} \quad \eta_T \\
 0^{++} \text{ technisigma} \quad \sigma_T
 \end{array} \right\} , \quad (2.26)$$

all with masses on the order of the technicolor scale $\Lambda_{TC} \sim O(1 \text{ TeV}/c^2)$, since they do not originate as Goldstone bosons. The dominant decay of the technirho will be

$$\rho_T \rightarrow \pi_T \pi_T , \quad (2.27)$$

i.e., into pairs of longitudinally polarized gauge bosons. Standard estimates lead to

$$\begin{aligned}
 M(\rho_T) &\approx 1.77 \text{ TeV}/c^2 \\
 \Gamma(\rho_T) &\approx 325 \text{ GeV}
 \end{aligned} \quad (2.28)$$

2.2.3 Extended technicolor. Technicolor shows how the generation of intermediate boson masses could arise without fundamental scalars or unnatural adjustments of parameters. It thus provides an elegant solution to the naturalness problem of the standard model. However, it has a major deficiency: it offers no explanation for the origin of quark and lepton masses, because no Yukawa couplings are generated between Higgs fields and quarks or leptons.

A possible approach to the problem of quark and lepton masses is suggested by "extended technicolor" models. We imagine that the technicolor gauge group is embedded in a larger extended technicolor gauge group,

$$G_{TC} \subset G_{ETC} , \quad (2.29)$$

which couples quarks and leptons to the technifermions. If the ETC symmetry is spontaneously broken down to the TC symmetry

$$G_{ETC} \rightarrow G_{TC} , \quad (2.30)$$

at a scale

$$\Lambda_{ETC} \sim 30 - 300 \text{ TeV} , \quad (2.31)$$

then the quarks and leptons may acquire masses

$$m \sim \Lambda_{TC}^3 / \Lambda_{ETC}^2 . \quad (2.32)$$

The outlines of this strategy are given in References 12 and 13, but no “standard” ETC model has been constructed.

As a representative of the ETC strategy we may consider a model due to Farhi and Susskind.^{14]} Their model is built on new fundamental constituents, the techniquarks

$$\begin{pmatrix} U \\ D \end{pmatrix}_L \quad U_R \quad D_R , \quad (2.33)$$

which are analogs of the ordinary quarks, and the technileptons

$$\begin{pmatrix} N \\ E \end{pmatrix}_L \quad N_R \quad E_R , \quad (2.34)$$

which are analogs of the ordinary leptons. These technifermions are bound by the $SU(N)_{TC}$ gauge interaction, which is assumed to become strong at $\Lambda_{TC} \sim 1 \text{ TeV}$. Among the $F\bar{F}$ bound states are eight color-singlet, technicolor-singlet pseudoscalar states [labeled by (I, I_3)]

$$\begin{array}{lcl}
\left. \begin{array}{l} \pi_T^+ (1,1) \\ \pi_T^0 (1,0) \\ \pi_T^- (1,-1) \end{array} \right\} & \text{become longitudinal } W^\pm \text{ and } Z^0 & \\
\left. \begin{array}{l} P^+ (1,1) \\ P^0 (1,0) \\ P^- (1,-1) \\ P^{0'} (0,0) \end{array} \right\} & \text{pseudo-Goldstone bosons} & \\
\eta_T' (0,0) & \text{techniflavor singlet} &
\end{array} \tag{2.35}$$

plus the corresponding technivector mesons. Like the η' of QCD, the η_T' couples to an anomalous current, so it is expected to acquire a mass on the order of several hundred GeV/c^2 . The pseudo-Goldstone bosons are massless in the absence of electroweak and ETC interactions.

Eichten, Hinchliffe, Lane, and I examined the possibilities for studying the light particles implied in such a model with the current generation of accelerators.^{15]} In the absence of extended-technicolor interactions, the neutral technipions P^0 and $P^{0'}$ remain massless, while the charged technipions P^+ and P^- acquire electroweak masses of a few GeV/c^2 . When ETC interactions are included, the technipion masses have been estimated as^{13,16]}

$$\begin{aligned}
8 \text{ GeV}/c^2 < M(P^\pm) < 40 \text{ GeV}/c^2 \\
2 \text{ GeV}/c^2 < M(P^0, P^{0'}) < 40 \text{ GeV}/c^2
\end{aligned} \tag{2.36}$$

If, as expected in the simplest models of Higgs bosons, the couplings of pseudoscalars into fermion pairs are proportional to fermion mass, the dominant decay modes will be

$$\begin{aligned}
P^+ &\rightarrow t \bar{b} \text{ or } c \bar{b} \text{ or } c \bar{s} \text{ or } \tau^+ \nu \\
P^0 &\rightarrow b \bar{b} \text{ or } c \bar{c} \text{ or } \tau^+ \tau^- \\
P^{0'} &\rightarrow b \bar{b} \text{ or } c \bar{c} \text{ or } \tau^+ \tau^- \text{ or } gg
\end{aligned} \tag{2.37}$$

Despite the possible similarities between Higgs bosons and technipions, there are important distinguishing characteristics. First, in the standard model, there is a direct HZZ coupling in the Lagrangian, whereas in the

Farhi-Susskind model the P^0ZZ coupling is induced through the triangle anomaly. As a consequence, we would expect the decay of a virtual $Z^* \rightarrow ZH$ to be about four orders of magnitude stronger than that of $Z^* \rightarrow ZP^0$. If a Higgs-like entity is seen in the reaction

$$e^+e^- \rightarrow Z^0 \rightarrow Z^{0*} \begin{matrix} \searrow \\ \hookrightarrow \ell^+\ell^- \end{matrix} \quad (2.38)$$

then it is the Higgs, and technicolor is ruled out. Second, in a multi-Higgs model, the decay $Z^0 \rightarrow H^0 H^{0'}$ is allowed (although the rate depends on details, such as mixing angles). In contrast, the decay $Z^0 \rightarrow P^0 P^{0'}$ is inhibited; we therefore expect

$$\Gamma(Z^0 \rightarrow P^0 P^{0'}) \ll \Gamma(Z^0 \rightarrow H^0 H^{0'}) \quad (2.39)$$

A clear presentation of the differences between Higgs bosons and technipions is given in Reference 17.

2.2.4 Colored technipions. From the color triplet ($U D$) and color-singlet ($N E$) technifermions, we may build $^1S_0 (F\bar{F})$ states:

- an isospin triplet P_3^1, P_3^0, P_3^{-1} of color triplets;
- an isospin singlet, color triplet state P_3' ;
- the corresponding antitriplet states;
- an isospin triplet P_8^+, P_8^0, P_8^- of color octets;
- an isoscalar color-octet state P_8^0 ,

with masses (acquired from the color interaction) of

$$\begin{aligned} M(P_3) &\approx 160 \text{ GeV}/c^2 \\ M(P_8) &\approx 240 \text{ GeV}/c^2 \end{aligned} \quad (2.40)$$

With standard charge assignments for the technifermions, the P_3 and P_3' charges are $(5/3, 2/3, -1/3; 2/3)$.

Pairs of colored technipions will be produced with substantial cross sections at supercollider energies, principally by gluon fusion. As an example, I show in Figure 1 the integrated cross section for the reaction

$$pp \rightarrow P_3 \bar{P}_3 + \text{anything} , \quad (2.41)$$

with and without the technirho ($\rho_8^{0'}$) enhancement. The expected decay modes of the color-triplet technipions are

$$P_3 \rightarrow q \bar{l} \text{ or } \bar{q} \bar{q} , \quad (2.42)$$

i.e., final states such as $t\tau^+$, tv_τ , $b\tau^+$, $\bar{t}\bar{b}$, etc. Production rates are substantial; the challenge will be to identify and measure the heavy-fermion decay products.

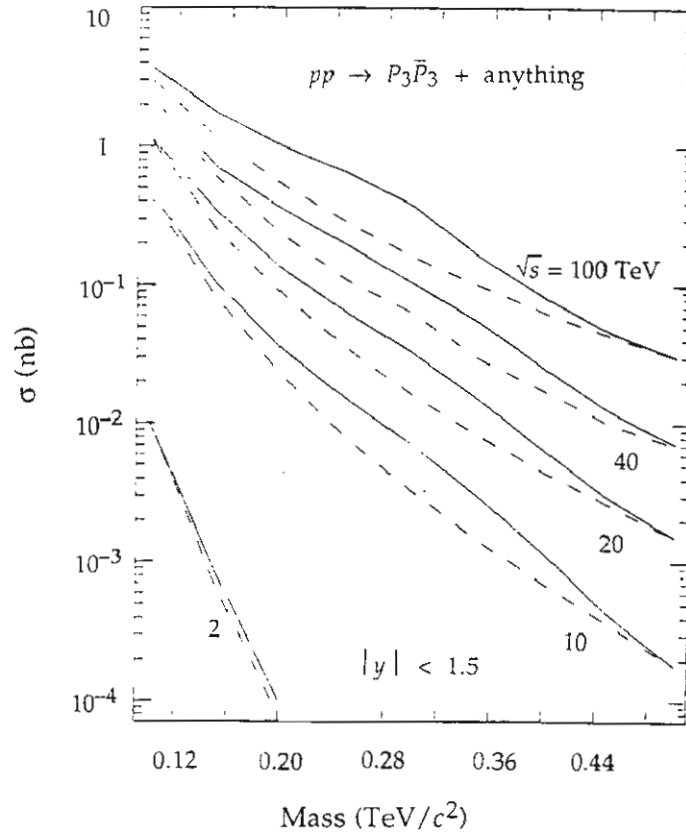


Figure 1: Integrated cross section for the production of $P_3 \bar{P}_3$ pairs in pp collisions, as a function of the P_3 mass (from EHLQ). Rapidities of the technipions must satisfy $|y| < 1.5$. The cross sections are shown with (solid lines) and without (dashed lines) the technirho enhancement. The expected mass of P_3 is around $160 \text{ GeV}/c^2$.

2.2.5 Appraisal. If the technicolor hypothesis correctly describes the breakdown of the electroweak gauge symmetry, there will be a number of spinless technipions with masses below the technicolor scale of about 1 TeV. In the simplest versions of technicolor, some of these—the color singlet, technicolor singlet particles—should be quite light (with masses $\lesssim 40 \text{ GeV}/c^2$) and could be studied using the current generation of e^+e^- and $\bar{p}p$ colliders. Similar light scalars arise in multiple Higgs models and in supersymmetry. The colored particles are probably inaccessible to experiment before a supercollider comes into operation, as are the technivector mesons. Full exploitation of the scientific opportunities requires the efficient identification and measurement of heavy quark flavors and—for the technivector mesons—the ability to identify intermediate bosons in complex events.

One of the vulnerabilities of technicolor models is that they do not naturally guarantee the absence of flavor-changing neutral currents. In “walking technicolor” models,^{18]} in which the $SU(N)_{TC}$ coupling evolves very slowly over a large range of momenta above Λ_{TC} , it appears possible to suppress flavor-changing neutral currents. A secondary consequence would be to increase the masses of the lightest technipions to about $100 \text{ GeV}/c^2$.

I am frequently asked what effect high-critical-temperature oxide superconductors will have on elementary-particle physics. The questioner usually has in mind potential applications of a miraculous new substance to the technology of particle accelerators. This is an interesting area for speculation and dreaming, but I submit that it misses the truly revolutionary opportunities presented by the phenomenon of 1-2-3 superconductors. The common thread of the progress in elementary-particle physics over the past twenty-five years has been the shameless exploitation of ideas appropriated from condensed-matter physics. The Ginzburg-Landau theory is none other than the nonrelativistic limit of the Abelian Higgs model, which opened the way to our understanding of spontaneous breaking of gauge symmetries. We have just seen that technicolor theories draw inspiration from the BCS theory. In this light, the implications of oxide superconductors for particle physics should be obvious to any ambitious young theorist. What we must do is identify the correct theory of high- T_c superconductors ... and steal it!

3. SOME HADRON COLLIDER DISCOVERY POSSIBILITIES

We have seen that the standard model hints that the frontier of our ignorance lies at about 1 TeV for collisions among the fundamental constituents. This conclusion is specific to electroweak symmetry breaking, which is important and can be phrased sharply, but is not the only interesting issue we face. More generally, the success of our theoretical framework suggests that a significant step is needed to see breakdowns of the standard model. Hadron colliders opening unexplored territory offer a broad range of discovery possibilities. Let us consider a few examples.

3.1 New Gauge Bosons

There are many reasons to be open to the possibility of new gauge bosons:

- high-energy parity restoration in an electroweak gauge theory based on the symmetry group $SU(2)_L \otimes SU(2)_R \otimes U(1)_Y$;
- the occurrence of extra $U(1)$ gauge symmetries, implying additional Z^0 s, for example in unification groups larger than $SU(5)$;
- the low-energy gauge groups emerging from superstring models.

In a specific theory, the calculation of W^\pm and Z^0 production rates is easily modified to yield an estimate of the cross section for the production of new gauge bosons. As an example, I show in Figure 2 the cross section for the production of a new W -boson with standard gauge couplings to the light quarks. For the 40-TeV energy projected for the SSC, we may anticipate sensitive searches out to a mass of about $6 \text{ TeV}/c^2$.

The exceptional group E_6 has a long history as a candidate group for the unification of the strong, weak, and electromagnetic interactions. Historically, the motivation for considering E_6 derived mainly from the observation that E_6 is the group beyond $SO(10)$, which is in turn the group beyond $SU(5)$:

$$E_6 \supset SO(10) \supset SU(5) . \quad (3.1)$$

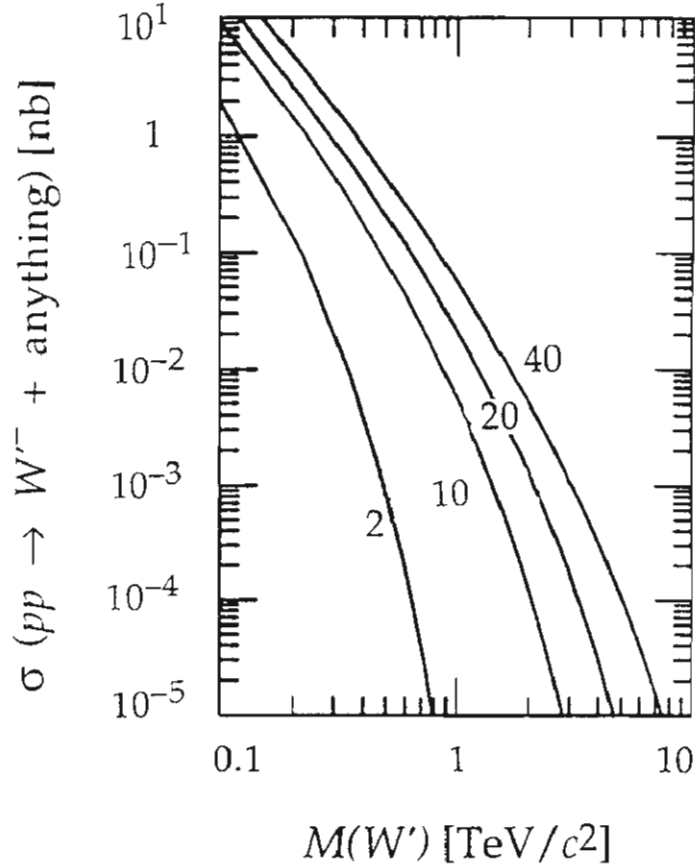


Figure 2: Cross section for the production of a heavy W -boson with rapidity $|\eta| < 1.5$ in pp collisions at 2, 10, 20, and 40 TeV (after EHLQ).

The current revival is owed to the possibility that E_6 may be the surviving symmetry of the $E_8 \otimes E_8'$ internal symmetry group of the heterotic string.^{19]} Like all applications of superstring ideas to phenomenology, the “derivation” of E_6 is very vague and tentative. Nevertheless, it provides us with a reason to look again at some possible consequences of an E_6 gauge symmetry.

With respect to interactions, we are interested in a scheme for spontaneous symmetry breaking that will lead eventually to the low-energy symmetry $SU(3)_c \otimes SU(2)_L \otimes U(1)_Y$. Thus we wish to break

$$E_6 \rightarrow \cdots \rightarrow SU(3)_c \otimes SU(2)_L \otimes U(1)_Y [\otimes \mathcal{G}] , \quad (3.2)$$

where \mathcal{G} denotes possible additional symmetries that survive to low energies. There are examples in superstring theories of symmetry breaking

induced by an E_6 adjoint 78 of Higgs bosons. This leads naturally to one or more extra $U(1)$ factors at low energies, which in turn implies an extra gauge boson, Z' , coupled to a new conserved current corresponding to the charge $Q^{(\eta)}$.

The Z' is somewhat harder to produce in $p^\pm p$ collisions than a standard Z^0 of the same mass, because the couplings to light quarks are inhibited. The branching ratio for the decay into charged leptons, for example, is

$$\Gamma(Z' \rightarrow e^+ e^-) \approx 3\%/n_g, \quad (3.3)$$

where n_g is the number of generations, which is somewhat smaller (by about $1/n_g$) than that of the conventional Z^0 . The production cross sections for the new Z' are shown in Figure 3. We expect to be sensitive to this new object in the lepton pair channel for masses as large as about 3–4 TeV/ c^2 at the SSC.

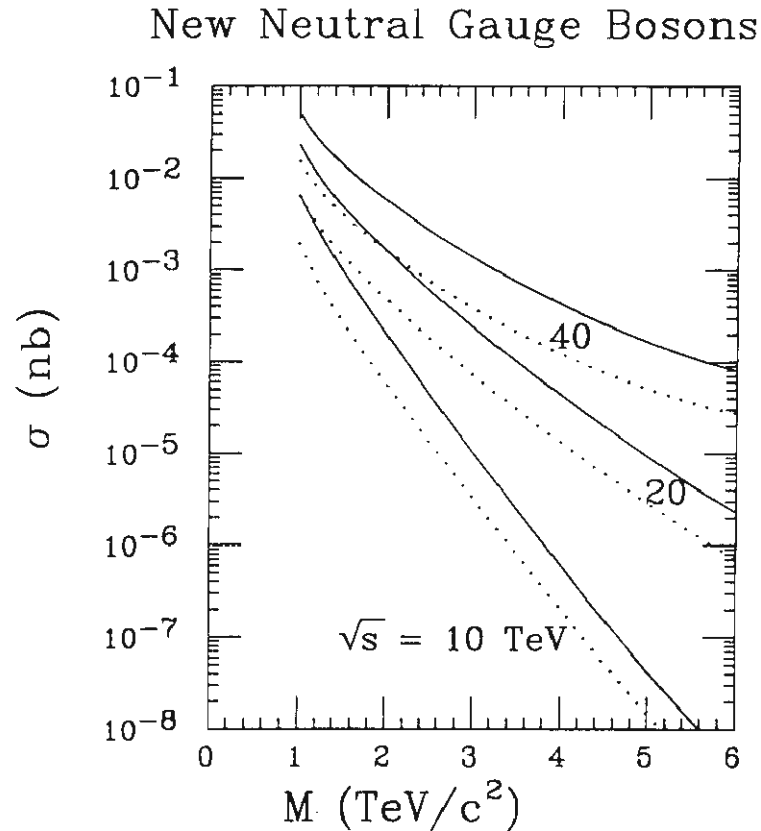


Figure 3: Cross section for the production of a heavy $Z^{0'}$ -boson with rapidity $|y| < 1.5$ in pp collisions at 10, 20, and 40 TeV. Solid lines: Weinberg-Salam couplings; dotted lines: E_6 couplings.

3.2 Sources of Heavy Quarks

Prominent sources of heavy quarks are strong-interaction production in the reactions $gg \rightarrow Q\bar{Q}$ and $q\bar{q} \rightarrow Q\bar{Q}$ and electroweak production through the decays of W^\pm and Z^0 . The latter have the advantage of known cross sections—which is to say cross sections that can be measured from the leptonic decays of the gauge bosons—and calculable branching ratios. However, they lead to very large rates only for the decays of real (not virtual) gauge bosons. This makes them an attractive option for the top-quark search at the SppS and at the Tevatron.

The cross sections for the strong interaction processes are known in QCD perturbation theory:²⁰¹ Under most circumstances, the process $gg \rightarrow Q\bar{Q}$ is dominant and the reaction $q\bar{q} \rightarrow Q\bar{Q}$ makes a negligible contribution. I show in Figure 4 the yield of heavy quarks from these sources at the SSC.

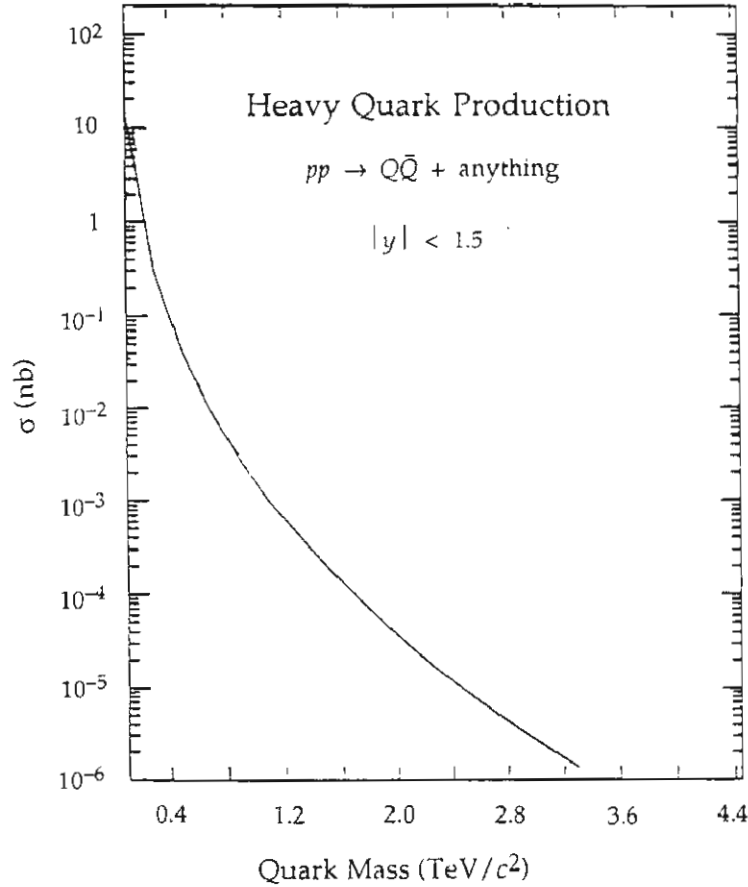


Figure 4: Integrated cross section for pair production of heavy quarks satisfying $|y_Q|, |y_{\bar{Q}}| < 1.5$ in pp collisions at 40 TeV.

There we expect an event rate sufficient for the discovery of heavy quarks with masses up to about $2 \text{ TeV}/c^2$. An evaluation of the requirements for detection depends upon the decay chain. If the dominant decay of the heavy quark is

$$Q \rightarrow t + W^- , \quad (3.4)$$

as it is likely to be, the ultimate decay products will be different if the top-quark mass is greater or less than the mass of the intermediate boson.

3.3 Two-Jet Events

In a hadronic collision, useful kinematic variables are p_{\perp} , the transverse momentum of either jet, and the jet rapidities

$$y_i = \frac{1}{2} \log \left(\frac{E+p_z}{E-p_z} \right) , \quad (3.5)$$

where p_z is the component of jet momentum along the beam direction. The dominant characteristic of many of these reactions is an angular dependence

$$\frac{d\sigma}{d\cos\theta^*} \sim \frac{1}{(1-\cos\theta^*)^2} , \quad (3.6)$$

arising from the t -channel gluon exchange, analogous to the t -channel photon exchange that drives the Rutherford formula. In terms of the variable $\chi \equiv \cot^2(\theta^*/2)$, the angular distribution may be reexpressed as

$$\frac{d\sigma}{d\chi} \sim \text{constant} . \quad (3.7)$$

The angular distribution of two-jet events in the dijet c.m. frame, for dijets with effective masses in the interval

$$150 \text{ GeV}/c^2 < \mathcal{M}(\text{jet-jet}) < 250 \text{ GeV}/c^2 , \quad (3.8)$$

has been measured by the UA1 collaboration.^{21]} To first approximation, the distribution is flat in χ , as our simple analogy with Rutherford scattering would suggest. In more detail, it agrees very precisely with the prediction of

the parton model. This is representative of the degree to which the expectations of QCD are being checked in collider experiments.

Once we can trust in the predictions of QCD in detail, it becomes increasingly interesting to search for deviations from the standard model. The idea that the quarks and leptons are structureless, indivisible elementary particles is basic to our current understanding. Testing the elementarity of quarks and leptons is therefore high on the agenda for future experiments. If the quarks are composite, they can interact not only by exchanging gluons, but also through the interchange of their constituents. As Eichten, Lane, and Peskin have pointed out,^{22]} for (anti)quark-(anti)quark collisions at energies approaching the compositeness scale Λ^* , the effect of this new reaction mechanism is to introduce a contact term of geometrical size into the scattering amplitude.

I show in Figure 5 the differential cross section $d\sigma/dp_{\perp} dy|_{y=0}$ for the reaction

$$p p \rightarrow \text{jet} + \text{anything} \quad (3.9)$$

at 40 TeV, for elementary quarks ($\Lambda^* = \infty$) and for quarks composite on scales of 10, 15, and 20 TeV. The gross features of these curves are easily understood. Because the contact term modifies the cross section for (anti)quark-(anti)quark scattering, its effects are most apparent at the large values of p_{\perp} for which valence quark interactions dominate the cross section. At 40 TeV and an integrated luminosity of 10^{40} cm^{-2} , SSC experiments will be able to probe scales of 15–20 TeV. Detailed measurements of the jet-jet angular distribution should extend the range of sensitivity. The first run of the CDF experiment at the Fermilab Tevatron, at an energy of $\sqrt{s} = 1.8 \text{ TeV}$, has set a lower limit of about 0.7 TeV on the scale of quark compositeness.^{23]}

3.4 Pairs of Gauge Bosons

Incisive tests of the structure of the electroweak interactions may be achieved in detailed measurements of the cross sections for the production of W^+W^- , $W^{\pm}Z^0$, Z^0Z^0 , $W^{\pm}\gamma$, and $Z^0\gamma$ pairs. The rate for $W^{\pm}\gamma$ production is sensitive to the magnetic moment of the intermediate boson. In the standard model there are important cancellations in the amplitudes for W^+W^-

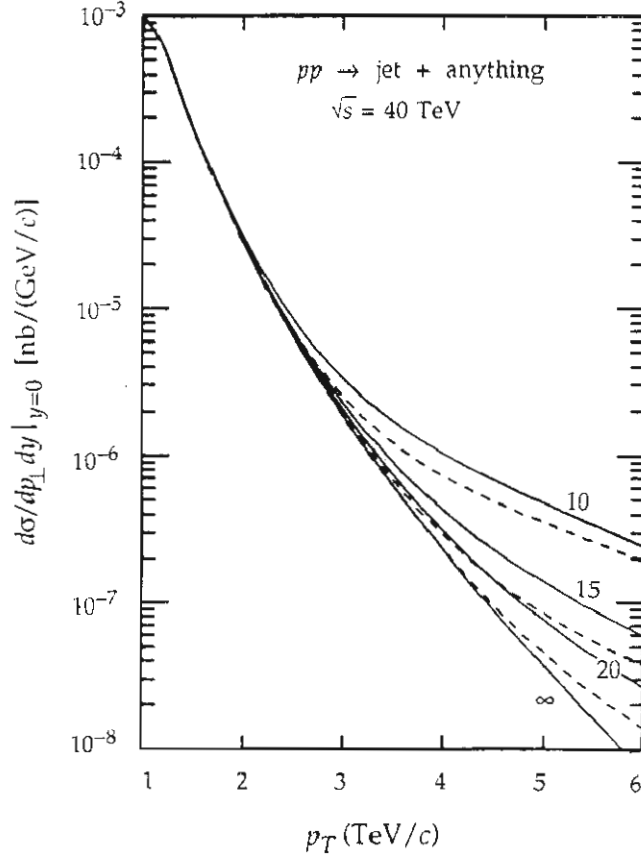


Figure 5: Differential cross section $d\sigma/dp_{\perp}dy|_{y=0}$ for the reaction $pp \rightarrow \text{jet} + \text{anything}$ at 40 TeV. The curves are labeled by the compositeness scale Λ^* (in TeV). Solid (dashed) lines indicate constructive (destructive) interference between the QCD amplitude for (anti)quark-(anti)quark scattering and the contact term.

and $W^{\pm}Z^0$ production that rely on the gauge structure of the WWZ trilinear coupling. The Z^0Z^0 and $Z^0\gamma$ reactions do not probe trilinear gauge couplings in the standard model, but they are sensitive to nonstandard interactions such as might arise if the gauge bosons were composite. In addition, the W^+W^- and Z^0Z^0 final states may be significant backgrounds to the detection of heavy Higgs bosons and possible new degrees of freedom.

The intrinsic interest in the process $q_i\bar{q}_i \rightarrow W^+W^-$, which accounts in part for plans to study e^+e^- annihilations at c.m. energies around 180 GeV at LEP, is owed to the sensitivity of the cross section to the interplay among the γ , Z^0 , and quark-exchange contributions. In the absence of the Z^0 -exchange term, the cross section for production of a pair of longitudinally polarized intermediate bosons is proportional to E_{cm}^2 , in gross violation of unitarity. It

is important to verify that the amplitude is damped as expected. The mass spectrum of W^+W^- pairs is of interest both for the verification of gauge cancellations and for the assessment of backgrounds to heavy Higgs boson decays. This is shown for intermediate bosons satisfying $|y| < 2.5$ in Figure 6. The number of pairs produced at high energies seems adequate for a test of the gauge cancellations, provided that the intermediate bosons can be detected with high efficiency.

Table 1 shows the expected yields of pairs of electroweak gauge bosons at the $S\bar{p}pS$, the Tevatron, and the SSC. At 630 GeV and an integrated luminosity of $10^{37} \text{ cm}^{-2} = 10 \text{ pb}^{-1}$, prospects for the study of W^+W^- pairs are remote. It may be barely possible to initiate studies at 1.8 TeV and $10^{38} \text{ cm}^{-2} = 100 \text{ pb}^{-1}$. At 40 TeV and $10^{40} \text{ cm}^{-2} = 10^4 \text{ pb}^{-1}$, we can look forward to 2×10^6 W^+W^- pairs per year. Efficient detection is the key to incisive studies.

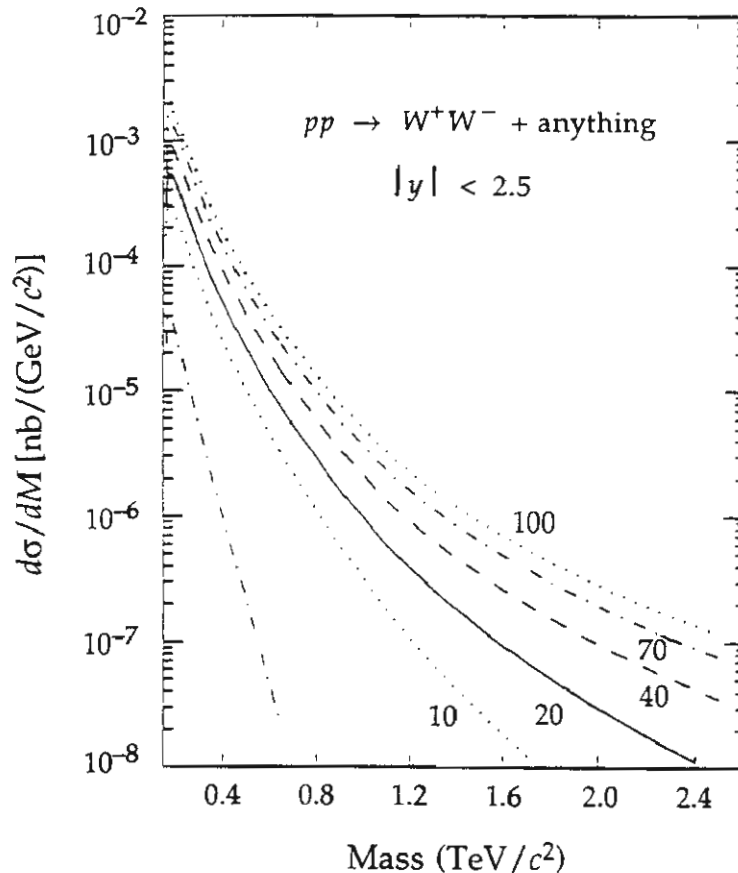


Figure 6: Mass spectrum of W^+W^- pairs produced in pp collisions at 40 TeV, according to the standard model and Set 2 of the EHLQ parton distributions. Both the W^+ and the W^- must satisfy $|y| < 2.5$.

Table 1: Cross sections (in pb) for pair production of electroweak gauge bosons.

Pair	630 GeV $\bar{p}p$	1.8 TeV $\bar{p}p$	40 TeV pp
W^+W^-	0.43	6.4	214
$W^\pm Z^0$	0.51	1.65	73
Z^0Z^0	0.034	0.074	33

3.5 The Higgs Boson

We have already remarked that the standard model does not give a precise prediction for the mass of the Higgs boson. We can, however, use arguments of self-consistency to place plausible lower and upper bounds on the mass of the Higgs particle in the minimal model. A lower bound is obtained by computing^{24]} the first quantum corrections to the classical potential

$$V(\phi^\dagger \phi) = \mu^2(\phi^\dagger \phi) + |\lambda|(\phi^\dagger \phi)^2. \quad (3.10)$$

Requiring that $\langle \phi \rangle \neq 0$ be an absolute minimum of the one-loop potential yields the condition

$$\begin{aligned} M_H^2 &> 3G_F\sqrt{2}(2M_W^4 + M_Z^4 - 3m_t^4)/16\pi^2 \\ &\geq 7.2 \text{ GeV}/c^2 \end{aligned} \quad (3.11)$$

where the numerical estimate is made for $m_t = 39 \text{ GeV}/c^2$.

Unitarity arguments^{25]} lead to a conditional upper bound on the Higgs-boson mass. It is straightforward to compute the s -wave partial-wave amplitudes for gauge-boson scattering at high energies in the

$$W^+W^- \quad Z^0Z^0 \quad HH \quad Z^0H \quad (3.12)$$

channels. These are all asymptotically constant (i.e., well-behaved) and proportional to $G_F M_H^2$. Requiring that the Born diagrams respect the partial-wave unitarity condition $|a_0| \leq 1$ yields

$$M_H^2 < \left(\frac{8\pi\sqrt{2}}{3G_F} \right) = (1 \text{ TeV}/c^2)^2 \quad (3.13)$$

as a condition for perturbative unitarity. Recent studies^{26]} of the consistency of lattice versions of the standard model suggest that an upper bound on the Higgs mass may be in the neighborhood of $700 \text{ GeV}/c^2$.

A heavy Higgs boson (by which we mean one with $M_H > 2M_Z$) will have the characteristic signature of decay into a pair of gauge bosons, with branching fraction roughly $2/3$ into the W^+W^- channel and $1/3$ into the Z^0Z^0 channel. Event rate permitting, the simplest mode in which to detect a heavy Higgs boson is the four-charged-lepton final state arising from the decay chain

$$H^0 \rightarrow \begin{array}{c} Z^0 \quad Z^0 \\ \downarrow \quad \downarrow \\ \ell^+\ell^- \quad \ell^+\ell^- \end{array} \quad (3.14)$$

The most promising mechanisms for Higgs-boson production are the gluon fusion process and the intermediate-boson fusion process. The rate for gluon fusion is sensitive to the masses of the quarks circulating in the loop, particularly to the top-quark mass. I show in Figure 7 for various Higgs-boson masses the yield of Z^0Z^0 events detected through the cascade (3.14) in the reaction $pp \rightarrow H^0 + \text{anything}$. The signal becomes less distinct at high masses, both because the number of events decreases and because the Higgs-boson width is proportional to $G_F M_H^3$. The SSC should nevertheless allow us to carry out a thorough search for a heavy Higgs boson for masses up to $1 \text{ TeV}/c^2$.

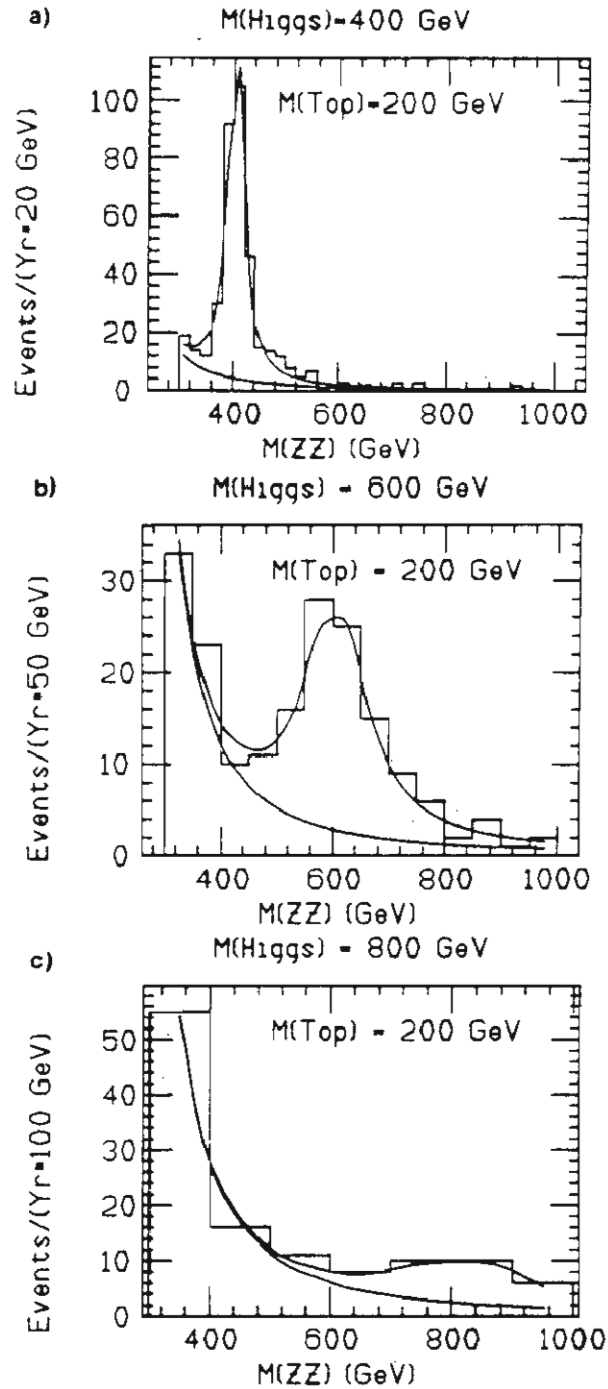


Figure 7: The ZZ invariant mass distribution arising from the production and decay of a Higgs boson in the reaction $pp \rightarrow H + \text{anything}$, and from the background process $q\bar{q} \rightarrow ZZ$ at $\sqrt{s} = 40$ TeV with an integrated luminosity of 10^{40} cm⁻². Both gauge bosons must satisfy the cut $|y_i| < 1.5$. The top-quark mass is taken to be 200 GeV/ c^2 , and perfect resolution and detection efficiency is assumed for both electrons and muons (from Ref. 27).

4. EXPERIMENTAL ENVIRONMENT OF THE SSC

Signals and backgrounds for specific phenomena at the SSC have been studied extensively, and quite fruitfully, over the past four years.^{1, 28–33]} In addition, it is important to be aware of the general environment in which SSC detectors must function and events must be selected and recorded. The basic parameters of the SSC are set out in the Conceptual Design Report,^{34]} a non-site-specific conception of a $20 \oplus 20$ TeV proton-proton collider 84 km in circumference. The design calls for two clusters of interaction regions incorporating both physics experimental areas and major supporting equipment. At the design luminosity of $10^{33} \text{ cm}^{-2}\text{sec}^{-1}$, interactions will occur at the rate of

$$0.016 \cdot (\sigma_t/1 \text{ mb}) \text{ interactions/crossing} . \quad (4.1)$$

The length of each bunch of protons is 6.0–7.3 cm, and adjacent bunches are separated by 4.8 m, or about 15 ns.

We expect the total cross section at 40 TeV to lie in the range

$$100 \text{ mb} \lesssim \sigma_t \lesssim 200 \text{ mb} , \quad (4.2)$$

so that the event rate at the design luminosity may range up to 2×10^8 per second. The current best guess for the total cross section^{35]} is $\sigma_t = 138 \text{ mb}$, of which about 92 mb is inelastic scattering.

A good way to gain respect for the conditions that will prevail at the SSC is to examine the trigger rate for events with transverse energy E_T greater than some threshold E_T^{min} . This is shown in Figure 8 for the nominal operating conditions of the SSC: $\sqrt{s} = 40 \text{ TeV}$ and $\mathcal{L} = 10^{33} \text{ cm}^{-2}\text{sec}^{-1}$, as well as at 10 and 100 TeV. At 40 TeV, a high- E_T trigger with threshold set at 2 TeV will count at 1 Hz from two-jet QCD events. This is of interest in planning triggers to efficiently select interesting events from the 2×10^8 interactions that will take place each second in an SSC interaction region.

The SSC experimental environment is complex and presents a challenge to technology for many aspects of detector components. This does not mean that we do not know how to build experiments for the SSC, but simply that we can profit from improvements in many areas of detector technology. There is time to carry out detector R&D that can yield rich rewards before designs of first-round experiments must be frozen.

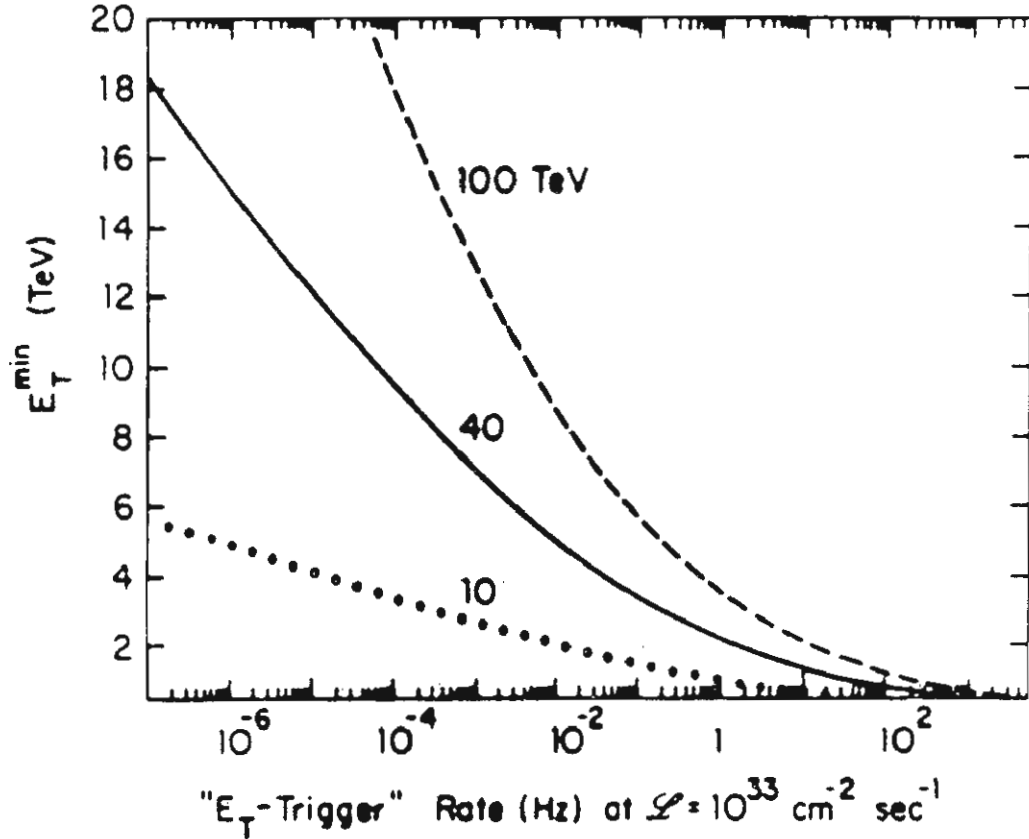


Figure 8: Counting rate for an E_T -trigger in pp collisions at an instantaneous luminosity of $\mathcal{L} = 10^{33} \text{ cm}^{-2} \text{ sec}^{-1}$. The threshold is defined for transverse energy deposited in the central region of rapidity, defined by $|y_i| < 2.5$ for jets 1 and 2.

Some of the desired improvements can be characterized as evolutionary. Electronic components of improved capability in smaller, cheaper packages can eliminate cables and enable us to place more computational discrimination and decision-making circuitry on the detector itself. More computing power per dollar means more capability and flexibility. It is easy to imagine that within a few years of initial operation the largest SSC experiments will be using computing power equivalent to one million VAX-11/780s.

Other technological improvements are directly driven by the physics goals of SSC experiments and by the high-luminosity environment. Some examples are fast, radiation-resistant silicon pixel detectors capable of resolving large particle densities and very large, well-calibrated, compensated

calorimetry systems that respond equivalently to electromagnetic and hadronic showers.

The initial goals of experimentation at the SSC help define detector issues that we should address vigorously:

- High-efficiency W and Z detectors will have great utility. The discovery physics we have considered in assessing the prospects of the SSC can all be done by relying upon the leptonic decays of the gauge bosons, but we can move to a deeper level of experimentation by learning to use the nonleptonic decays as well.
- The UA1 experiment has already indicated the value of "hermetic" detectors, which can capture and measure all the visible energy emitted in the central region. For a general-purpose SSC detector, it is of interest to require hermeticity for rapidities $|y| < 3$.
- Examples from technicolor and the Higgs sector of the standard model indicate that good-efficiency τ , b , ... tags will be of considerable value in enhancing signals over background. Full utilization of the heavy-flavor tag requires measuring the four-momenta of the short-lived particles as well.
- How to reduce the interaction rate of $\sim 10^8$ Hz to the rate ($O(1$ Hz)) at which complex events can be written on storage media (magnetic tapes, optical discs)? There are many opportunities for creativity here!
- Bringing remote local intelligence into the detector components themselves requires the implementation of radiation-hardened electronics, especially near the beam directions.

5. STATUS OF THE SSC PROJECT

The chief attributes of the SSC's superconducting collider rings and of the cascade of accelerators providing intense proton beams to them are set forth in the 1986 Conceptual Design Report.^{34]}

Superconducting magnets were chosen for the SSC for two reasons. First, they make possible confining fields three times as strong as those available with conventional iron magnets. More important, the electrical power requirements for a superconducting machine are far smaller than for a conventional accelerator. A conventional version of the SSC would consume 4 GW of electrical power; the SSC's average consumption will be about forty times smaller.

Even with the more intense fields made possible by superconducting magnets, the SSC will be an instrument of impressive size. In the engineering units appropriate to the problem, the bending radius is related to beam momentum and confining field by

$$\rho = \left(\frac{10}{3} \text{ km} \right) \cdot \left(\frac{p}{\text{TeV}/c} \right) / \left(\frac{B}{\text{tesla}} \right). \quad (5.1)$$

For a 20-TeV/ c beam in a confining field of 6.6 teslas, the SSC design field, the implied radius of curvature is $\rho \approx 10$ km. With allowance for the straight sections accommodating experimental areas, acceleration gear, etc., the circumference of the SSC will be about 84 km.

The proposed layout of the Supercollider is shown in Figure 9. Interaction halls cluster on the two gently curved sides of the collider ring. In this perspective the near cluster incorporates the injector complex, the radio-frequency accelerating system, beam absorbers, and two of the six interaction halls. The far cluster adds four more interaction halls, two of which will be reserved for development after research begins, according to current plans. The schematic enlargement of an interaction hall shows a detector surrounding the point at which two beams collide; the cross section to the right shows the position of the two superconducting magnet rings in the tunnel. The two independent rings for the proton beams will sit one atop the other, 70 cm apart.

The superconducting magnets essential for guiding the protons around the rings are made of two coils arranged to approximate a $\cos\theta$ current distribution. The inner coil has an inside diameter of 4 cm. The coils are wound of cable made from composite strands (23 in the inner coil, 30 in the outer) containing thousands of filaments—each about 6 μm in diameter—of a niobium-titanium alloy embedded in a copper matrix. The small filaments reduce the size of the paths available for eddy currents, as laminations do in a transformer. This helps minimize distortions of the dipole

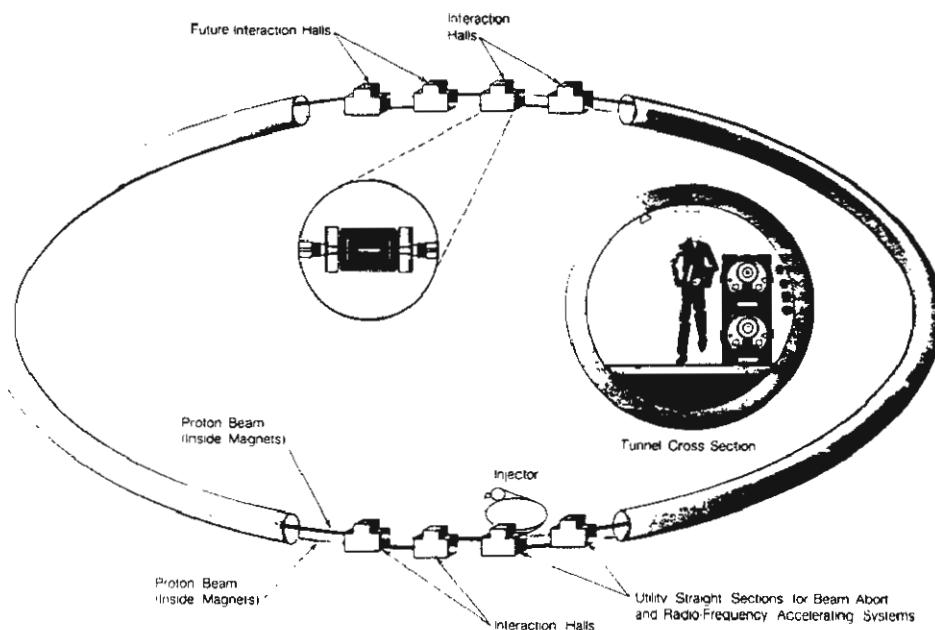


Figure 9: Collider ring layout envisaged in the SSC Conceptual Design Report.

confining field at injection, when the beam is most sensitive to field errors. Interlocking stainless steel or aluminum collars surrounded by an iron yoke hold the cables in place. This 17-meter-long package, called the "cold mass," is sealed in its own cryostat, where it can be maintained at an operating temperature of 4.35 K. The 3840 dipole magnets in each collider ring have a peak operating field of 6.6 teslas, which corresponds to a current of 6504 amperes. Figure 10 shows a cross section of the SSC dipole.

5.1 The Myth of a Boring Machine

I remarked at the beginning that the technical means to the study of the 1-TeV scale were not yet in hand when the importance of the 1-TeV scale was first recognized. The technical means to the SSC are themselves interesting and were unforeseen only a short time ago.

The development of new strategies for reaching higher energies has parallels in the development of new tools for optical astronomy. The 2.5-m telescope on Mount Wilson, with a mirror made of plate glass, began operation in 1917 and was the largest telescope in the world for thirty years. In the

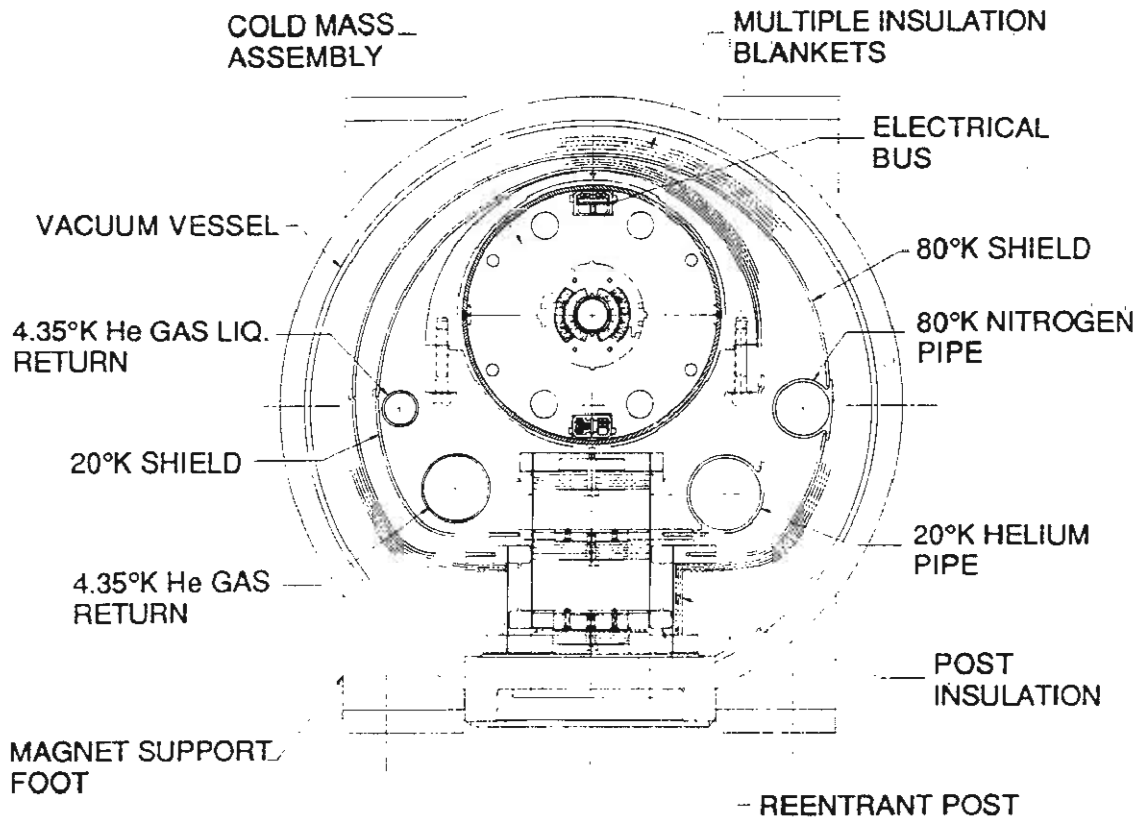


Figure 10: Cross section of the 6.6-tesla superconducting dipole magnet for the SSC.

1930s, the invention of Pyrex made practical the casting of a 5-m mirror for the Hale Telescope on Palomar Mountain, where observations began in 1949. Because of the difficulties in casting large mirror blanks, telescopes built since then—with the single exception of the 6-m Mount Pastukhov instrument in the Caucasus, commissioned in 1976—have all been substantially smaller. Advances have occurred in instrumentation, with electronic detectors replacing photographic plates and computer controls replacing manual pointing of the instrument. Telescopes at other locations expanded the portion of the sky we could study.

Recent inventions have broken the 5-m barrier. These include multiple-mirror telescopes, with effective apertures much larger than can be obtained efficiently with a single mirror; active optics, embodied in the idea of the so-called "rubber telescope" that corrects its figure in real time to respond to variations in the density of the column of air above it; segmented mirrors,

in which a mosaic of mirrors of manageable size is positioned under microprocessor control. New fabrication methods promise large, lightweight mirrors shaped in a spinning oven, like a potter's wheel, and mirrors with nonspherical surfaces, made by the technique of stressed-mirror polishing. Open-air telescopes minimize the aberrations caused by temperature gradients within the protective tube of traditional instruments.

These innovations, which are widely appreciated both by professional astronomers and by the interested public, all have analogs in the construction of proton accelerators for high-energy physics. Because developments in accelerator science and technology are not so well known, many of our colleagues who equate an accelerator with a spigot regard the SSC as a boring machine ("just a bigger Tevatron") and convey the dinosaur image to their students and to the public at large. Let me indicate briefly why they are mistaken.

A truly boring machine was the one conceived by Enrico Fermi in his farewell address as President of the American Physical Society in January, 1954. Fermi's dream machine was intended to produce a beam of 5000-TeV protons, comparable to the highest-energy cosmic-ray protons then known. It consisted of a ring of conventional (two-tesla) magnets circling the globe in low earth orbit at a radius of 8000 km. He estimated that such a device could be constructed by 1994 at a cost of \$170 billion. (Fermi's assumptions about inflation are not preserved.) Although the 3-TeV c.m. energy that could be reached in fixed-target experiments represented a great step from the energies of a few GeV the Bevatron would produce later in 1954, Fermi's machine was free of technical innovations.

What has happened in reality is much more interesting. Experience at CERN's ISR and SppS and at Fermilab's Tevatron confirms that the most efficient way to reach high c.m. energies is to construct high-intensity colliding beams of protons. Superconducting magnets achieve fields several times those produced by warm iron magnets, with a concomitant reduction in ring radius, and effect enormous savings in electric bills. Active optics to achieve real-time corrections of the orbits of particles in the accelerator has yielded the benefits of "cooling," or phase-space compaction, of stored antiproton beams and makes it possible to build reliable, highly tuned accelerators from magnets with small apertures, which are therefore cheaper. Cryogenic technology has advanced so rapidly that the refrigeration required for the SSC will be no greater than what was needed for the

Tevatron. Finally, advances in superconducting cable involving the production of homogeneous fine filaments of niobium-titanium alloy and manipulations of materials on essentially the atomic scale have led to increased field intensity and improved field quality, with corresponding cost reductions. As a result, the SSC will reach 160 times the equivalent laboratory energy envisaged by Fermi for a small fraction of the cost.

5.2 Since the Conceptual Design Report

The SSC design team has not been idle since the Conceptual Design Report was published two and a half years ago. Much effort has been devoted to elaborating the conceptual design, to inventing more elegant and cost-efficient solutions to design problems, and to developing detailed designs for the accelerator components. I will briefly mention a few areas in which important progress has been made.

5.2.1 Accelerator lattice. The design of the collider ring has been strengthened in two important ways since the Conceptual Design Report. A refined lattice,^{36]} in which the phase advance per cell is increased from the 60° of the CDR to 90° , results in increased tolerance for magnet imperfections, a larger effective dynamic aperture, and more compact dispersion suppressors, while maintaining great flexibility in the characteristics of the interaction regions. The space between interaction points is gently curved, so muons produced in beam-beam collisions at one interaction region are offset by 94 meters from the next collision point. Current concepts for the interaction regions will leave ± 20 m of free space for detectors in the high-luminosity ($\mathcal{L} = 10^{33} \text{ cm}^{-2}\text{sec}^{-1}$) areas and ± 120 m of free space in the intermediate-luminosity ($\mathcal{L} = 0.8\text{--}5.0 \times 10^{31} \text{ cm}^{-2}\text{sec}^{-1}$) areas. This work provides a firm foundation for the creation of a site-specific conceptual design; the configuration of the experimental areas will be determined by the scientific program the SSC laboratory develops in consultation with the user community.

Both simulations and experimental measurements have improved our understanding of the dynamic aperture for protons in a superconducting storage ring. The larger the diameter of the beam tube, the more expensive the superconducting magnet. Therefore there is strong incentive to select a magnet aperture that is as small as is consistent with graceful and reliable

operation of the machine. A formal accelerator experiment (Fermilab E-778) carried out on the Tevatron has added support to the CDR aperture choice and has yielded interesting physics results as by-products. Enhanced instrumentation capable of recording beam positions for up to 10^6 turns has made possible the direct observation³⁷¹ of resonance islands in the x versus x' phase space plot, or Poincaré section.

5.2.2 Superconducting cable. Substantial increases in the current-carrying capacity of superconducting cable have resulted from a collaboration among industry, universities, and the U.S. national laboratories focused on the development of improved superconductor for the SSC. The SSC specification for the critical current density in niobium-titanium strand, $J_c = 2750 \text{ A/mm}^2$ at 4.2 K and 5 T, represents a 50 percent improvement over the conductor used in the Tevatron. Material meeting this demanding specification is now routinely received in production quantities. A high-speed cabling machine has been developed and installed in industry.

5.2.3 Dipole magnet development. During FY 1988, sixteen short (1- and 1.8-m) model magnets have been made and measured, to test fabrication methods and to explore the performance of various lots of superconducting cable. Typically these models have reached the predicted "short-sample" current with minimal training under SSC operating conditions at 4.35 K. When the temperature is reduced to 1.8 K, to increase the current-carrying capacity of the cable and thereby to test more stringently the mechanical integrity of the magnet cold mass, these magnets have been excited to fields above 9 T. Field quality, expressed in terms of multipoles, has been satisfactory.

In the same period, six full-length (17-m) models have been manufactured and six have been tested. The principal design criteria—including design field intensity, field alignment and uniformity, heat load, maximum temperature excursion during a quench, minimal training, and training retention—have all been demonstrated. Significant improvements have been made in the mechanical support system for the coil, aided by increasingly precise instrumentation in the form of voltage taps and strain gauges to study the initiation and propagation of quenches and to

understand the mechanical properties of the magnets at all stages of thermal cycles, during normal excitation, and during quenching.

The most successful long magnet reached its short-sample current, slightly above the SSC operating point, without training at 4.3 K. When cooled to 3.2 K, it reached a field of 7.6 T, corresponding to the short-sample limit at that temperature. Further cooling resulted in no increase in quench current, indicating that the mechanical limits of the magnet structure had been found. For this magnet, those limits reside in the "ramp splice" between inner and outer coils. An improved support structure for that region has been designed and will be incorporated into magnets in the near future.

5.3 The Year Ahead

The \$100-million appropriation for SSC R&D in fiscal year 1989 gives us the opportunity to show that we are prepared to make an aggressive construction start in the following year. To invest this money wisely, we will have to move quickly to double the staff of the Central Design Group. After the site has been confirmed, an important order of business will be the creation of a site-specific conceptual design, making whatever accommodations and optimizations are appropriate. We shall also have to begin in earnest on the conceptual development of the injector accelerators and will have to consider scientific policy issues surrounding the pace at which the injectors are brought into operation. It is worth spending a few moments to summarize the kinds of R&D activities that will occupy our attention during the coming months.

In the area of accelerator theory, there will be continued studies of beam dynamics to settle on the final lattice for the collider rings and to help specify the requirements for the superconducting dipoles, quadrupoles, and correction elements. The development of operations simulation software is essential for determining the nature and optimal placement of diagnostic devices around the ring.

Since 1987 there has been a growing program of generic detector research and development germane to SSC experiments. In this year, approximately thirty universities, the five national high-energy physics laboratories

(Argonne, BNL, Fermilab, LBL, and SLAC), and Oak Ridge National Laboratory will be involved in about 55 separate detector R&D tasks relevant to the SSC. This very wide-ranging effort comprises work on

- advanced calorimetry, including hermetic design for liquid argon devices, warm liquid tests, scintillating fibers, silicon sampling, and improvements to shower codes;
- silicon tracking devices, including development of fast two-dimensional arrays or pixel devices, and studies of radiation damage;
- wire chambers, including investigations of radiation damage, studies of fast drift velocity gases, development of large arrays of straw tubes, and simulations;
- electronics, including integrated circuitry for drift chambers, calorimetry and silicon devices, studies of radiation damage, and development of radiation-hardened circuits;

and many other areas. A vigorous R&D effort in the next few years will lead naturally into preparations for specific SSC experiments and provide much of the technical basis for the initial SSC complement of detectors.

We will try to build on the improvements already realized in superconducting cable, stimulating the development of increased production capacity and working with industrial vendors to increase the yield of superconducting strand by increasing the diameter of the copper/niobium-titanium billets. Poisoning the copper matrix with 0.5 percent (by weight) of manganese has been shown in research billets to inhibit coupling between closely spaced superconducting filaments, reducing the effects of residual eddy currents that distort the dipole field at injection. It will be important to learn whether this property can be maintained in mass production. In preparation for the procurement of large quantities of cable in the years ahead, we must develop better and more efficient methods for measuring cable characteristics. Good progress has already been made on monitoring the size and shape of cable with high-speed measuring machines. This year will bring increased attention on high-field measurements of electrical characteristics.

The development of a final, manufacturable design of the dipole magnets will continue to take high priority. In addition to prototyping, testing, and developing tooling, we plan to expand our repertoire of mechanical and thermal modeling tools. The first phase of an industrialization program is under way with a technology orientation phase designed to acquaint potential industrial vendors with the lessons of the magnet R&D effort. We will continue preparing for systems (cell) tests to understand how strings of magnets behave under normal operating conditions and when quenches occur, and we will begin accelerated-life tests to search out weaknesses in the magnet design. Finally, we will begin to prototype the other magnets—quadrupoles, spool pieces, and correctors—that complete the accelerator lattice.

One of the first requirements of the new SSC laboratory will be for a Magnet Test Laboratory to evaluate magnets manufactured in industry and to enable continuing magnet R&D within the laboratory. The cryogenic specifications for an MTL are being developed, and we hope to commission a detailed engineering design and begin to order components this year.

In the realm of conventional construction, detailed geotechnical surveys will soon begin. Preliminary engineering and design of the collision halls must proceed quickly, so the final configuration and location of the ring can be determined in order that land acquisition can proceed on schedule.

This outline of some of the important work before us suggests the complexity of the effort and the great number of challenging tasks that talented people will have to assume in order to bring the dream of the SSC to reality.

When might the SSC be in operation? An important milestone was passed in March 1986, when the SSC Central Design Group completed the Conceptual Design Report for the SSC. Every major system had been thought through, and a detailed cost estimate had been made. Because a location had not been selected for the Supercollider, the Conceptual Design was not adapted for any specific site. During the summer of 1986, the Department of Energy and independent experts validated the cost and technical feasibility of the machine described in the Conceptual Design Report.

President Reagan endorsed the SSC as a national goal in January 1987. In April of that year, the Department of Energy began a site search that led to a short list of seven "Best Qualified Sites" in the states of Arizona, Colorado, Illinois, Michigan, North Carolina, Tennessee, and Texas. On November 10, 1988, Secretary of Energy John S. Herrington announced his choice of Waxahachie, Texas, 25 miles south of Dallas, as the preferred site for what will be called the Ronald Reagan Center for High-Energy Physics. From the time the site is available, sometime in 1989, it will take about seven and a half years to build the machine. We hope to commence experimentation with the SSC by 1996.

We believe that the SSC can foster a new level of international cooperation in particle physics. As a frontier research instrument, the Supercollider will certainly attract to its experimental program many of the best particle physicists from around the world. This is of course traditional in our field, but we may hope for more: active international collaborations established early enough to allow significant foreign participation in the design and construction of the SSC and its detectors, and not just in the performance of experiments.

The advances of the past decade have brought us tantalizingly close to a profound new conception of the most basic constituents of matter and their interactions. The simpler and more comprehensive understanding we have gained organizes current knowledge and locates the horizon of particle physics at energies of trillions of electron volts. Important answers will be found with the SSC: from it we await new discoveries about the unification of the forces of nature and the patterns of the fundamental constituents of matter.

ACKNOWLEDGMENTS

It is a pleasure to thank Peter Carruthers, Jan Rafelski, and all of our hosts in Tucson for their warm hospitality and efficient organization. Kate Metropolis made insightful comments on the manuscript and Valerie Kelly prepared the final version for publication. The SSC Central Design Group is operated by Universities Research Association, Inc., under contract with the U.S. Department of Energy.

FOOTNOTES AND REFERENCES

1. For a summary of the shortcomings of the standard model, see E. Eichten, I. Hinchliffe, K. D. Lane, and C. Quigg, *Rev. Mod. Phys.* **56**, 579 (1984); *ibid.* **58**, 1065E (1986).

2. M. Veltman, *Acta Phys. Pol. B* **12**, 437 (1981); C. H. Llewellyn Smith, *Phys. Rep.* **105**, 53 (1984).

3. Reviews of the experimental implications of supersymmetry on the scale of electroweak symmetry breaking appear in D. V. Nanopoulos and A. Savoy-Navarro (ed.), *Phys. Rep.* **105**, 1 (1984); H. E. Haber and G. L. Kane, *ibid.* **117**, 75 (1985); S. Dawson, E. Eichten, and C. Quigg, *Phys. Rev. D* **31**, 1581 (1985); R. M. Barnett, H. E. Haber, and G. L. Kane, *Nucl. Phys.* **B267**, 625 (1986).

4. For reviews of the technicolor idea, see E. Farhi and L. Susskind, *Phys. Rep.* **74**, 277 (1981); R. Kaul, *Rev. Mod. Phys.* **55**, 449 (1983). A study for the current generation of hadron colliders appears in E. Eichten, I. Hinchliffe, K. Lane, and C. Quigg, *Phys. Rev. D* **34**, 1547 (1986).

5. The idea of a strongly interacting gauge sector is an evergreen in particle theory. In the context of the standard model, early discussions appear in M. Veltman, *Acta Phys. Pol. B* **8**, 475 (1977) and B. W. Lee, C. Quigg, and H. B. Thacker, *Phys. Rev. D* **16**, 1519 (1977). Recent investigations appropriate to the supercollider scale are reported in M. Chanowitz and M. K. Gaillard, *Nucl. Phys.* **B261**, 379 (1985); *idem*, *Phys. Lett.* **142B**, 85 (1984); M. Chanowitz, M. Golden, and H. Georgi, *Phys. Rev. D* **36**, 1490 (1987).

6. V. L. Ginzburg and L. D. Landau, *Zh. Eksp. Teor. Fiz.* **20**, 1064 (1950).

7. J. Bardeen, L. N. Cooper, and J. R. Schrieffer, *Phys. Rev.* **106**, 162 (1962).

8. Y. Nambu, *Phys. Rev. Lett.* **4**, 380 (1960).

9. M. Weinstein, *Phys. Rev. D* **8**, 2511 (1973).

10. S. Weinberg, *Phys. Rev. D* **13**, 974 (1976), *ibid.* **19**, 1277 (1979).

11. L. Susskind, *Phys. Rev. D* **20**, 2619 (1979).

12. S. Dimopoulos and L. Susskind, *Nucl. Phys.* **B155**, 237 (1979).

13. E. Eichten and K. Lane, *Phys. Lett.* **90B**, 125 (1980).

14. E. Farhi and L. Susskind, *Phys. Rev. D* **20**, 3404 (1979).

15. Eichten, et al., Ref. 4.

16. V. Baluni, *Phys. Rev. D* **28**, 2223 (1983); *Ann. Phys. (NY)* **165**, 148 (1985).
17. K. D. Lane, in *Proceedings of the 1982 DPF Summer Study on Elementary Particle Physics and Future Facilities*, edited by R. Donaldson, R. Gustafson, and F. Paige (Fermilab, Batavia, Illinois, 1982), p. 222.
18. T. Appelquist and L. C. R. Wijewardhana, *Phys. Rev. D* **36**, 568 (1987); for a recent review, see T. Appelquist, M. Soldate, T. Takeuchi, and L. C. R. Wijewardhana, Yale report YCTP-P19-88, to be published in the Proceedings of the 12th Johns Hopkins Workshop on Current Problems in Particle Theory, Baltimore, June 9–10, 1988.
19. M. Green and J. Schwarz, *Phys. Lett.* **149B**, 117 (1984); *ibid.* **151B**, 21 (1985); D. J. Gross, J. A. Harvey, E. Martinec, and R. Rolm, *Phys. Rev. Lett.* **54**, 502 (1985); *idem*, *Nucl. Phys.* **B256**, 253 (1985); E. Witten, *Nucl. Phys.* **B258**, 75 (1985); M. Dine, V. Kaplunovsky, M. Mangano, C. Nappi, and N. Seiberg, *Nucl. Phys.* **B259**, 519 (1985).
20. B. L. Combridge, *Nucl. Phys.* **B151**, 429 (1979). The radiative corrections, not included in the estimates displayed in Figure 4, have been evaluated by P. Nason, S. Dawson, and R. K. Ellis, *Nucl. Phys.* **B303**, 607 (1988).
21. G. Arnison, et al. (UA1 collaboration), *Phys. Lett.* **177B**, 244 (1986).
22. E. Eichten, K. Lane, and M. E. Peskin, *Phys. Rev. Lett.* **50**, 811 (1983).
23. M. J. Shochet, Rapporteur's talk at the XXIV International Conference on High Energy Physics, Munich, August, 1988.
24. A. D. Linde, *Pis'ma Zh. Eksp. Teor. Fiz.* **23**, 73 (1976) [*JETP Lett.* **23**, 64 (1976)]; S. Weinberg, *Phys. Rev. Lett.* **36**, 294 (1976).
25. Lee, Quigg, and Thacker, Ref. 5.
26. For upper bounds on the Higgs-boson mass deduced from lattice field theory studies of the standard model, see J. Kuti, L. Lin, and Y. Shen, *Phys. Rev. Lett.* **61**, 678 (1988); G. Bhanot and K. Bitar, *ibid.* **61**, 798 (1988).
27. R. N. Cahn, et al., in *Proceedings of the Workshop on Experiments, Detectors, and Experimental Areas for the Supercollider*, Berkeley, 1987, edited by R. Donaldson and M. G. D. Gilchriese (World Scientific, Singapore, 1988), p. 20.
28. *Large Hadron Collider in the LEP Tunnel*, edited by G. Brianti, et al., CERN 84-10.

29. *Proceedings of the 1984 Summer Study on Design and Utilization of the Superconducting Super Collider*, edited by R. Donaldson and J. G. Morfín (Fermilab, Batavia, Illinois, 1984); *$\bar{p}p$ Options for the Supercollider*, edited by J. E. Pilcher and A. R. White (University of Chicago, 1984); *Physics at the Superconducting Super Collider Summary Report*, edited by P. Hale and B. Winstein (Fermilab, 1984).

30. *Supercollider Physics*, edited by D. E. Soper (World Scientific, Singapore, 1986).

31. *Proceedings of the Summer Study on the Physics of the Superconducting Super Collider, Snowmass, 1986*, edited by R. Donaldson and J. Marx (Division of Particles and Fields of the American Physical Society, New York, 1987).

32. *Les Rencontres de Physique de la Vallée d'Aoste, Results and Perspectives in Particle Physics*, edited by M. Greco (Editions Frontières, Gif-sur-Yvette, France, 1987).

33. *Proceedings of the Workshop on Experiments, Detectors, and Experimental Areas for the Supercollider*, Berkeley, 1987, edited by R. Donaldson and M. G. D. Gilchriese (World Scientific, Singapore, 1988).

34. *Superconducting Super Collider Conceptual Design*, Central Design Group Report SSC-SR-2020 (March, 1986).

35. M. M. Block and R. N. Cahn, in *Proceedings of the 2nd International Conference on Elastic Scattering and Diffractive Processes*, Rockefeller University, October, 1987, edited by K. Goulianos (Editions Frontières, Gif-sur-Yvette, France, 1988), p. 88.

36. A. A. Garren and D. E. Johnson, "The 90° (September 1987) SSC Lattice," SSC-146. A full parameter list is forthcoming.

37. A. W. Chao, et al., "Experimental Investigation of Nonlinear Dynamics at the Tevatron," submitted to *Phys. Rev. Lett.*